

# Dielectric and thermal evidence of phase transitions in the system of $(1 - x)\text{Pb}(\text{Mg}_{1/3}\text{Nb}_{2/3})\text{O}_3 - x\text{PbTiO}_3$ crystals

Cite as: Appl. Phys. Lett. **90**, 252902 (2007); <https://doi.org/10.1063/1.2710077>

Submitted: 28 November 2006 . Accepted: 24 January 2007 . Published Online: 19 June 2007

Haixia Wang, Xiaomin Pan, Di Lin, Haosu Luo, Zhiwen Yin, and Brahim Elouadi



View Online



Export Citation

## ARTICLES YOU MAY BE INTERESTED IN

[Ultrahigh strain and piezoelectric behavior in relaxor based ferroelectric single crystals](#)

Journal of Applied Physics **82**, 1804 (1997); <https://doi.org/10.1063/1.365983>

[Electric-field-induced and spontaneous relaxor-ferroelectric phase transitions in  \$\(\text{Na}\_{1/2}\text{Bi}\_{1/2}\)\_{1-x}\text{Ba}\_x\text{TiO}\_3\$](#)

Journal of Applied Physics **112**, 124106 (2012); <https://doi.org/10.1063/1.4770326>

[Piezoelectric properties and temperature stability of Mn-doped  \$\text{Pb}\(\text{Mg}\_{1/3}\text{Nb}\_{2/3}\)\text{-PbZrO}\_3\text{-PbTiO}\_3\$  textured ceramics](#)

Applied Physics Letters **100**, 132908 (2012); <https://doi.org/10.1063/1.3698157>



**Measure Ready**  
**M91 FastHall™ Controller**

A revolutionary new instrument for complete Hall analysis

Lake Shore  
CRYOTRONICS

## Dielectric and thermal evidence of phase transitions in the system of $(1-x)\text{Pb}(\text{Mg}_{1/3}\text{Nb}_{2/3})\text{O}_3-x\text{PbTiO}_3$ crystals

Haixia Wang<sup>a)</sup>

Shanghai Institute of Ceramics, Chinese Academy of Sciences, 215 Chenbei Rd. Jiading, Shanghai 201800, China; Laboratoire d'Elaboration Chimique et Ingénierie des Matériaux, Université de La Rochelle, avenue Michel Crépeau, 17042 La Rochelle Cédex 01, France; and Graduate School of the Chinese Academy of Sciences, Beijing 100039, China

Xiaomin Pan, Di Lin, Haosu Luo, and Zhiwen Yin

Shanghai Institute of Ceramics, Chinese Academy of Sciences, 215 Chengbei Rd. Jiading, Shanghai 201800, China

Brahim Elouadi<sup>b)</sup>

Laboratoire d'Elaboration Chimique et Ingénierie des Matériaux, Université de La Rochelle, avenue Michel Crépeau, 17042 La Rochelle Cédex 01, France

(Received 28 November 2006; accepted 24 January 2007; published online 19 June 2007)

Dielectric permittivity, differential scanning calorimetry nonisothermal measurements, and hysteresis loops were performed for oriented  $(1-x)\text{Pb}(\text{Mg}_{1/3}\text{Nb}_{2/3})\text{O}_3-x\text{PbTiO}_3$  unpoled crystals. Two distinguished branches were obtained where spontaneous ferroelectric to relaxor or ferroelectric phase transition was observed within the peculiar relaxor to normal ferroelectric region. The percolating polar region induced by the addition of  $\text{PbTiO}_3$  tends to gradually develop comparable ferroelectric order changing slightly with temperature from the nonpolar matrix, associated with a weak first or first order phase transition. Small frequency dispersion due to relaxor polarization at or below transition temperature  $T_{\text{FE-R}}$  or  $T_{\text{FE}}$  indicated the changes of ferroelectric multidomain and polar nanoregion in this disordered system. © 2007 American Institute of Physics. [DOI: 10.1063/1.2710077]

Both single crystals and ceramics of the lead-based solid solution such as  $(1-x)\text{Pb}(\text{Mg}_{1/3}\text{Nb}_{2/3})\text{O}_3-x\text{PbTiO}_3$ , i.e., PMN-PT,  $x$ : molecular content, have been recognized to endorse outstanding physical properties with potential and effective technological applications in various fields as transducers, sensors, actuators, etc.<sup>1,2</sup> Since the pioneering work of Smolenskii and Agranouskaya,<sup>4,5</sup> all structural studies have concluded that PMN and related systems adopt the perovskite structure. Many investigations have evidenced structural deformations changing with composition  $x$  and giving rise to different types of lattice such as rhombohedral, monoclinic, orthorhombic, and tetragonal with a general agreement that the high temperature prototype is always of a cubic symmetry.<sup>3,6-8</sup> The previous reports tend to confirm the tendency to reduce the relaxor behavior of pure PMN with increasing  $x$  as the system progresses from PMN to normal ferroelectric PT. It is worth to mention that despite almost five decades of intensive and continuous investigations since the discovery of the relaxor character of the PMN-PT system, the nature of phase equilibria and phase transitions is still a hot subject.<sup>9</sup> The purpose of the present work is to give our contribution to the understanding of the phase diagram of the title system. Indeed, investigating phase transitions in single crystals is very important which might not give the same phenomena as their ceramic counterparts.<sup>10</sup> Numerous discussions have evidenced that mixed oxide PMN-PT crystals exhibit more complex phase evolutions and have different symmetries when applying electric field along different

crystallographic directions.<sup>3,8</sup> No more conspicuous dielectric anomaly can be found near the ferroelectric-relaxor (FE-R) transition in unpoled PMN-PT system ( $x < 0.30$ ) except for  $x = 0.10$ .<sup>11,12</sup> This letter will focus on PMN-PT unpoled single crystals which show systematically dielectric and thermal anomalies evidenced by low frequency dielectric measurements coupled with differential scanning calorimeter (DSC) analysis.

The as-grown PMN-PT crystals ( $0 \leq x \leq 0.45$ ) using a modified Bridgman technique<sup>13</sup> was oriented along  $\langle 111 \rangle$  direction (considered as a pseudocubic phase) by x-ray diffractometer, and then the wafer (about  $8 \times 8 \times 0.7 \text{ mm}^3$ ) was diced and covered by calcined silver. The local compositions (about  $10 \mu\text{m}$ ) at different positions of the polished transparent specimens free from visible structural defects<sup>14</sup> were determined by energy dispersive spectrometer (INCA Energy, Oxford) together with electron-probe x-ray microanalysis (EPMA-8705QH<sub>2</sub>, Shimadzu, Japan). Small compositional fluctuations within  $\pm 0.9$  atomic mol % on small scales for the same sample would be resolved. The complex dielectric permittivity was investigated from 70 to 470 K at the heating rate of 1 K/min, using a liquid nitrogen bath cryostat (Oxford on DN1704, ITC601 temperature controller) and an HP4192A impedance analyzer at 0.01–10 kHz. The hysteresis ( $P$ - $E$ ) loops were recorded using a Sawyer-Tower circuit at 1 Hz and different temperatures. Heat flux DSC nonisothermal measurements (DSC-TA instrument Q10) allowed to record phase transitions under  $\text{N}_2$  atmosphere from 170 to 670 K at different heating rates. Crystalline samples around 10 mg were sealed in an aluminum cell while the calibration was initially achieved with a sharp peak ( $T = 433 \text{ K}$ ) of pure indium.

<sup>a)</sup>Electronic mail: salienca@hotmail.com

<sup>b)</sup>Author to whom correspondence should be addressed; electronic mail: belouadi@univ-lr.fr

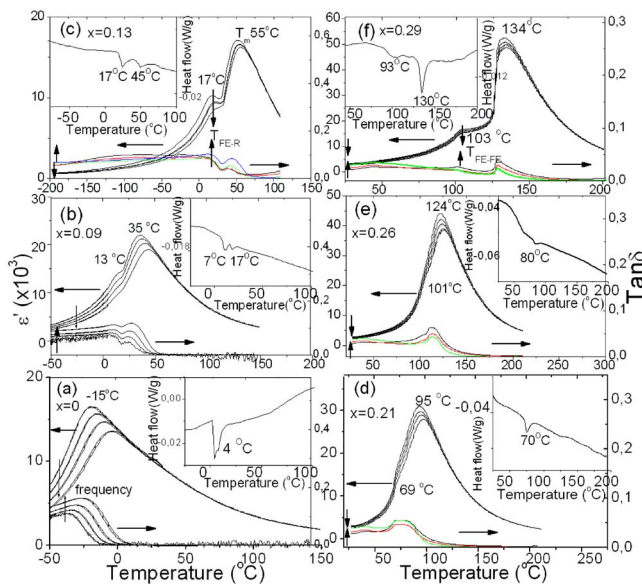


FIG. 1. (Color online) Thermal plots of the dielectric constant and dielectric loss for  $\langle 111 \rangle$ -oriented PMN-PT unpoled crystals: (a)  $x=0$ , (b)  $x=0.09$ , (c)  $x=0.13$ , (d)  $x=0.21$ , (e)  $x=0.26$ , and (f)  $x=0.29$ , with a heating rate of 1 K/min at different frequencies of 0.01, 0.6, 1.0, and 10 kHz, respectively (arrow: increasing frequency). Inset: DSC curves and the onset temperature obtained for each sample upon heating at the rate of 5 K/min (Exo. up).

Typical examples of thermal plots of the dielectric constant  $\epsilon'$  and dielectric loss  $\tan \delta$  of  $\langle 111 \rangle$ -oriented PMN-PT ( $0 \leq x \leq 0.03$ ) unpoled single crystals are shown in Fig. 1. In each curve the temperature  $T_m$  at the maximum  $\epsilon'_m$  of relative permittivity is in good agreement with previous results of the phase diagram associated with the ergodic relaxor phase or ferroelectric-paraelectric (PE) phase transition.<sup>3,5</sup> For PMN both plots of  $\epsilon'(T)$  and  $\tan \delta(T)$  in Fig. 1(a) evidence characteristics of canonical relaxors (where the anomalies of the structure and properties are diffused or lacking).<sup>3-6</sup> Moreover, the most remarkable result is the evidence of a second dielectric anomaly at temperature  $T < T_m$  in both curves of  $\epsilon'(T)$  and  $\tan \delta(T)$  for compositions  $x > 0$ . The jumps of dielectric response at  $T < T_m$  could be induced by a spontaneous FE-R transition in the heating process.<sup>12</sup> As expected for a relaxor behavior, the magnitude of  $\epsilon'_m$  decreases with increasing frequency and tends to stabilize at frequencies higher than 10 kHz. This is probably due to the damped dielectric response to the rotation of the polar nanoregions (PNRs) as in normal relaxors which have a long relaxation time. In Figs. 1(b) and 1(c), the peaks of dissipation factor tend to be sharper and the magnitudes increase with rising frequencies. However, the spontaneous FE-R transition temperature  $T_{FE-R}$  appears totally independent of frequency unlike  $T_m$ , as clearly shown for  $x=0.13$  [Fig. 1(c)]. A former work on unpoled single crystals ( $x=0.1$ ) has shown that  $T_{FE-R}$  peaks slightly change with the crystallographic directions<sup>12</sup> which do not exist anymore for  $x \geq 0.13$ .<sup>9</sup> It is clear that the spontaneous FE-R can be well induced upon the addition of PT up to 0.13. In Figs. 1(d) and 1(e),  $\epsilon'(T)$  characteristics for the FE-R transition were almost smeared and weak inflections appear a little diffused; however, there is no significant dispersion in the magnitude of  $\epsilon'$  with frequency unlike PMN. The diffuseness is attributed to a distribution of transformations, where  $T_{FE-R}$  and  $T_m$  tend to merge together. Note the breadth of dielectric loss peak in this case. Frequency independent  $T_{FE-R}$  in the dielectric loss still re-

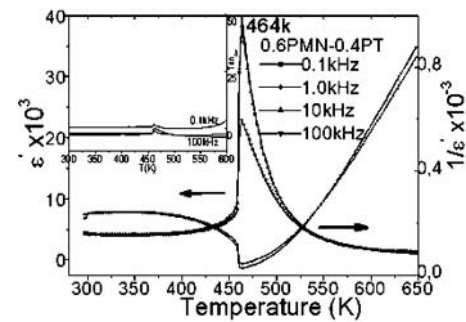


FIG. 2. Variation of dielectric constant  $\epsilon'_r(T, f)$ ,  $1/\epsilon'_r(T, f)$ , and dielectric loss (inset) of PMN-PT unpoled crystals ( $x=0.40$ ) at different frequencies.

mains and the magnitude dispersion of dielectric loss with two close inflections was symmetric around the loss peak. As  $x$  approaches the morphotropic phase boundary (MPB), such as  $x=0.29$  [Fig. 1(f)],  $T_{FE-R}$  and  $T_m$  with sharp peaks tend to be normal ferroelectric transformations, where the temperatures for the peaks of  $\epsilon'(T)$  and  $\tan \delta(T)$  were frequency independent and the magnitude of  $\tan \delta$  at and above  $T_{FE-R}$  or  $T_m$  decreased with increasing frequency similar to normal ferroelectrics for  $x \geq 0.38$  (Fig. 2). Therefore, the following phase transition sequences appear:

$$375 \text{ K} \quad 408 \text{ K}$$

FE  $\rightarrow$  FE  $\rightarrow$  PE. As the PMN-PT system changes from PMN to MPB, the dielectric characteristics at the lower temperature side of  $T_m$  exhibit the change from continuous to discontinuous.

It is very satisfying to notice that phase transitions evidenced from the dielectric plots are at the same temperature regions determined by the DSC analysis (see insets of Fig. 1). Phase transition temperatures allow to display a deduced phase diagram (Fig. 3), where the general feature is close to the literature for the PMN-PT system ( $0 \leq x \leq 0.45$ ) (Refs. 3 and 15–20) within the temperature range  $100 \text{ K} < T < 600 \text{ K}$ . The previous phase diagrams<sup>7,18,19</sup> show only one branch for  $x < 0.35$  whereas Fig. 3 exhibits two distinguished temperature branches ( $T_1 = T_m$  and  $T_2 = T_{FE-R}$  or FE) running almost parallel up to  $x=0.33$ . Disclosure of such effects is probably due to the fact that it was carried out on single crystals which allowed change of the orientation of the polar microdomains and PNRs.<sup>11</sup>

The composition within  $x=0.33-0.35$  described<sup>2,7</sup> to be MPB seems to play a particular role in the PMN-PT solid solution. Indeed, in Fig. 3 this region is related to the disap-

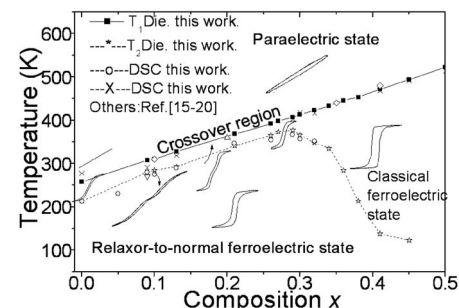


FIG. 3. Phase diagram of  $(1-x)\text{PMN}-x\text{PT}$  system deduced from the dielectric and DSC data, respectively.  $T_2$  points for  $x > 0.35$  come from poled PMN-PT crystals under 1 kV/mm (Ref. 15), others for unpoled PMN-PT crystals from this letter. The data from literatures (Refs. 16–20) are also shown for comparison.



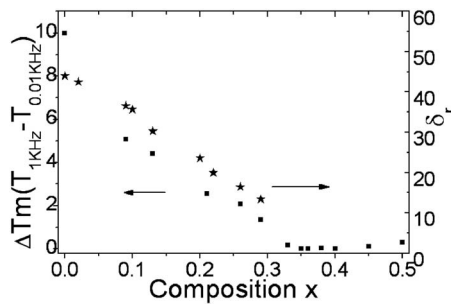


FIG. 4. Plot of  $\Delta T_m$  between frequencies of 0.01 and 1 kHz as a function of composition (left) and diffuse parameter  $\delta_r$  deduced from the power law (right).

pearance of  $T_2$  in unpoled PMN-PT crystals. Furthermore, it is worth to underline that for  $x > 0.35$ ,  $T_m$  does not change anymore with frequency as evidenced from Fig. 4. Particularly, as shown in Fig. 2 the curves of  $1/\epsilon'_r(T)$  exhibit frequency independent  $T_m$  and imply a typically first order phase transition. Therefore,  $T_m$  become a true Curie temperature  $T_C$ , i.e.,  $T_m = T_C$  for  $x > 0.35$ , and the title system behaves as a normal ferroelectric phase.

The plot of sequence hysteresis loops at  $T < T_C$  is a signal that the PMN-PT crystals behave characteristic of the ferroelectric state. For  $0.35 < x < 1$  square  $P$ - $E$  loops can be observed below  $T_C$  (Fig. 3),<sup>21</sup> which correspond to the existence of classical ferroelectrics. This transition with a typically first order nature has no diffuse character or double  $P$ - $E$  loop above  $T_C$  like in PT. However, with the composition decreasing to  $x=0$ , one observed the evolution of normal square to double and then a slimly nonlinear hysteresis loop (Fig. 3) between  $T_{FE-R}$  or  $T_{FE}$  and  $T_m$ , which allow the appearance of the sequence of normal ferroelectric state, the coexistence of ferroelectric and relaxor behavior with diffuse phase transition (DPT) and frequency dispersion at  $T_m$ , and the typical relaxor ferroelectric state in the peculiar crossover region. It does occur that the typical combination of FE-R characteristics is located at around  $x=0.21$  in the course of relaxor to normal FE state. Dielectric loss decreases and then increases with rising frequencies at the regions of  $T_{FE-R}$  and  $T_m$ , while small frequency dispersion at  $T_m$  still remains [Fig. 1(d)]. In fact,  $\epsilon'_r(T, f)$  characteristic related to DPT at  $T \geq T_m$  can be described according to the variable power law  $\epsilon'_m/\epsilon'(f, T) = 1 + [T - T_m(f)]^r / 2\delta_r^2$  ( $1 \leq r \leq 2$ ).<sup>5,22</sup> The values of  $\delta_r$  and  $r$  are regarded as a measure of degree of the diffuseness and dielectric relaxation in relaxor ferroelectrics, respectively.  $\epsilon'_r(T, f)$  obey the derivative equation well within the same temperature region ( $T_m \leq T \leq T_m + 70$  K) where there is a weak frequency dependence for  $\delta_r$  but no more correlation with frequency for  $r$ . Compared with PMN ( $r=2$ ), the crystals with higher  $x$  have lower values of  $r$  and  $\delta_r$  ( $r \approx 1.63$  for  $x=0.29$ , see Fig. 4) which implies weak degree of diffuseness and relaxor behavior. The PMN-PT system behaves similar to ferroelectrics with DPT for  $x > 0.13$  rather than to typical relaxors due to the still strong DPT and weak frequency dispersion.

It was argued that the critical behavior at  $T_C$  thermal hysteresis will not certainly imply a first order phase transition in highly disordered PMN-PT ceramics ( $x=0.25$ ) without discontinuous jump at  $T_C$  in  $\epsilon'_r(T)$  curves.<sup>23</sup> It almost happens in the same manner here especially for  $0.20 < x < 0.28$ , but spontaneous FE-R phase transition was still ob-

served at  $T < T_m$  upon heating in the plots of  $\tan \delta(T)$ . For the PMN-rich side the Curie-Weiss law of linear  $1/\epsilon'_r(T)$  relation at different frequencies is also satisfied at  $T < T_m$  (Ref. 9) as in normal ferroelectrics usually considered as a the second order phase transition. However, first order phase transition allows the coexistence of two phases at a temperature a little above  $T_C$  which is not permitted for the second order one. Furthermore, the continuous decrease of remnant polarization  $P_r$  versus temperature  $T$  and the absence of the electric field induced phase transition (where electric displacement is expressed as a monotonic function of electric field at  $T \geq T_C$ ) indicate a second order phase transition. Therefore, the sharp drop of  $P_r(T)$  at about  $T_{FE-R}$  and the appearance of double hysteresis above  $T_{FE-R}$ , for instance,  $x=0.21$  [see EPAPS (Ref. 24)], could be evidences of a first or weak first order phase transition in PMN-rich unpoled crystals at  $T_{FE-R} = T_C$ . A disturbed ferroelectric nature may occur although single  $P$ - $E$  loops (Fig. 3) appear below  $T_{FE-R}$ , where competence of local polar and long order of relaxor to normal FE region and the crystal structure imperfections do exist. Thus, small dielectric frequency dispersion may appear in the polar phase due to the relaxation of domain walls in this disordered system at  $T < T_{FE-R}$ .

The work was supported by NSF, China (Grant Nos. 50432030 and 50331040), the Shanghai Municipal Government (Grant No. 05JC14079), the Innovation Funds from CAS (SCX200411), and the French Embassy in China.

<sup>1</sup>R. E. Newhham, Q. C. Xu, S. Kumar, and L. E. Cross, *Ferroelectrics* **102**, 259 (1990).

<sup>2</sup>S. E. Park and T. R. Shrout, *J. Appl. Phys.* **82**, 1804 (1997).

<sup>3</sup>Z.-G. Ye, *Key Eng. Mater.* **155-156**, 81 (1998).

<sup>4</sup>G. A. Smolenskii and A. I. Agranouskaya, *Sov. Phys. Tech. Phys.* **3**, 1380 (1958).

<sup>5</sup>G. A. Smolenskii, *J. Phys. Soc. Jpn.* **28**, 26 (1970).

<sup>6</sup>L. E. Cross, *Ferroelectrics* **151**, 305 (1994).

<sup>7</sup>B. Noheda, D. E. Cox, G. Shirane, J. Gao, and Z.-G. Ye, *Phys. Rev. B* **67**, 064102 (2003).

<sup>8</sup>H. Cao, J. Li, D. Viehland, and G. Xu, *Phys. Rev. B* **73**, 184110 (2006).

<sup>9</sup>H. Wang, Ph. D. thesis, Chinese Academy of Sciences, 2007.

<sup>10</sup>P. Bao, F. Yan, W. Li, Y. R. Dai, H. M. Shen, J. S. Zhu, Y. N. Wang, H. L. W. Chan, and C.-L. Choy, *Appl. Phys. Lett.* **81**, 2059 (2002).

<sup>11</sup>Eugene V. Colla, Nikolai K. Yushin, and D. Viehland, *J. Appl. Phys.* **83**, 3298 (1998).

<sup>12</sup>H. Wang, H. Xu, H. Luo, Z. Yin, A. A. Bokov, and Z.-G. Ye, *Appl. Phys. Lett.* **87**, 012904 (2005).

<sup>13</sup>S.-H. Luo, G.-S. Shen, P.-C. Wang, X.-H. Le, and Z.-W. Yin, *J. Inorg. Matter.* **12**, 768 (1997).

<sup>14</sup>G.-S. Xu, H. Luo, H. Xu, Z. Qi, P. Wang, W. Zhong, and Z. Yin, *J. Cryst. Growth* **222**, 202 (2001).

<sup>15</sup>X. Wan, Ph.D. thesis, Chinese Academy of Sciences, 2005.

<sup>16</sup>B. Dkhil, J. M. Kiat, G. Calvarin, G. Baldinozzi, S. B. Vakhruhev, and E. Suard, *Phys. Rev. B* **65**, 024104 (2001).

<sup>17</sup>Z.-G. Ye, Y. Bing, J. Gao, A. A. Bokov, P. Stephens, B. Noheda, and G. Shirane, *Phys. Rev. B* **67**, 104104 (2003).

<sup>18</sup>M. H. Lente, A. L. Zanin, E. R. M. Andreeta, I. A. Santos, D. Garcia, and J. A. Eiras, *Appl. Phys. Lett.* **85**, 982 (2004).

<sup>19</sup>P. M. Gehring, S. Wakimoto, Z.-G. Ye, and G. Shirane, *Phys. Rev. Lett.* **87**, 277601 (2001).

<sup>20</sup>A. Slodczyk, A. Kania, Ph. Daniel, and A. Ratuszna, *J. Phys. D* **38**, 2910 (2005).

<sup>21</sup>H. Cao, B. Fang, H. Qin, and H. Luo, *Mater. Res. Bull.* **37**, 2135 (2002).

<sup>22</sup>K. Uchino and S. Nomura, *Ferroelectr., Lett. Sect.* **44**, 55 (1982).

<sup>23</sup>A. A. Bokov and Z.-G. Ye, *Appl. Phys. Lett.* **77**, 1888 (2000).

<sup>24</sup>See EPAPS Document No. E-APPLAB-90-090708 for hysteresis loops. This document can be reached via a direct link in the online article's HTML reference section or via the EPAPS homepage (<http://www.aip.org/pubservs/epaps.html>).